A dust-enshrouded tidal disruption event with a resolved radio jet in a galaxy merger

S. Mattila[1,2*†], M. Pérez-Torres[3,4*†], A. Efstathiou[5], P. Mimica[6], M. Fraser[7,8], E. Kankare[9], A. Alberdi[3], M. Á. Aloy[6], T. Heikkilä[1], P.G. Jonker[10,11], P. Lundqvist[12], I. Martí-Vidal[13], W.P.S. Meikle[14], C. Romero-Cañizales[15,16], S. J. Smartt[9], S. Tsygankov[1], E. Varenius[13,17], A. Alonso-Herrero[18], M. Bondi[19], C. Fransson[12], R. Herrero-Illana[20], T. Kangas[1,21], R. Kotak[1,9], N. Ramírez-Olivencia[3], P. Väisänen[22,23], R.J. Beswick[17], D.L. Clements[14], R. Greimel[24], J. Harmanen[1], J. Kotilainen[2,1], K. Nandra[25], T. Reynolds[1], S. Ryder[26], N.A. Walton[8], K. Wiik[1], G. Östlin[13]

[1]Tuorla Observatory, Department of Physics and Astronomy, University of Turku, Väisäläntie 20, 21500, Piikkiö, Finland.

[2]Finnish Centre for Astronomy with ESO (FINCA), University of Turku, Väisäläntie 20, 21500, Piikkiö, Finland.

[3]Instituto de Astrofísica de Andalucía - Consejo Superior de Investigaciones Científicas (CSIC), PO Box 3004, 18008, Granada, Spain.

[4]Departamento de Física Teórica, Facultad de Ciencias, Universidad de Zaragoza, 50019, Zaragoza, Spain.

[5]School of Sciences, European University Cyprus, Diogenes Street, Engomi, 1516 Nicosia, Cyprus.

[6]Department d'Astronomia i Astrofisica, Universitat de València Estudi General, 46100 Burjassot, València, Spain.

[7]School of Physics, O'Brien Centre for Science North, University College Dublin, Belfield, Dublin 4, Ireland.

[8]Institute of Astronomy, University of Cambridge, Madingley Road, Cambridge, CB3 0HA, UK.

[9]Astrophysics Research Centre, School of Mathematics and Physics, Queen's University Belfast, Belfast BT7 1NN, UK.

[10]SRON, Netherlands Institute for Space Research, Sorbonnelaan 2, NL-3584 CA Utrecht, the Netherlands.

[11]Department of Astrophysics, Institute for Mathematics, Astrophysics and Particle Physics, Radboud University, P.O. Box 9010, 6500GL Nijmegen, The Netherlands.

[12]Department of Astronomy and The Oskar Klein Centre, AlbaNova University Center, Stockholm University, SE-106 91 Stockholm, Sweden.

[13]Department of Space, Earth and Environment, Chalmers University of Technology, Onsala Space Observatory, SE-439 92 Onsala, Sweden.

[14]Astrophysics Group, Blackett Laboratory, Imperial College London, Prince Consort Road, London SW7 2AZ, UK.

[15]Millennium Institute of Astrophysics (MAS), Nuncio Monseñor Sótero Sanz 100, Providencia, Santiago, Chile.

[16]Núcleo de Astronomía de la Facultad de Ingeniería y Ciencias, Universidad Diego Portales, Av. Ejército 441, 8370191 Santiago, Chile.

[17]Jodrell Bank Centre for Astrophysics, The University of Manchester, Oxford Rd, Manchester M13 9PL, UK.

[18]Centro de Astrobiología (CSIC-INTA), ESAC Campus, E-28692 Villanueva de la Cañada, Madrid, Spain.

[19]Istituto di Radioastronomia - Istituto Nazionale di Astrofisica (INAF), Bologna, via P. Gobetti 101, 40129, Bologna, Italy.

[20]European Southern Observatory, Alonso de Córdova 3107, Vitacura, Casilla 19001, Santiago de Chile, Chile.

[21]Space Telescope Science Institute, 3700 San Martin Drive, Baltimore, MD 21218, US.

[22]South African Astronomical Observatory, PO Box 9, Observatory 7935, Cape Town, South Africa.

[23]Southern African Large Telescope, PO Box 9 Observatory 7935, Cape Town, South Africa.

[24]Institute of Physics, Department for Geophysics, Astrophysics, and Meteorology, NAWI Graz, Universitätsplatz 5, 8010 Graz, Austria.

[25]Max-Planck-Institut für extraterrestrische Physik, Giessenbachstraße, 85748, Garching, Germany.

[26]Australian Astronomical Observatory, 105 Delhi Rd, North Ryde, NSW 2113, Australia.

*Correspondence to: sepmat@utu.fi, torres@iaa.es

†These authors contributed equally to the work.

One-sentence summary:
We discovered an energetic tidal disruption event with an expanding radio jet and most of its energy radiated in the infrared.

Tidal disruption events (TDEs) are transient flares produced when a star is ripped apart by the gravitational field of a supermassive black hole (SMBH). We have observed a transient source in the western nucleus of the merging galaxy pair Arp 299 that radiated $>1.5\times10^{52}$ erg in the infrared and radio, but was not luminous at optical or X-ray wavelengths. We interpret this as a TDE with much of its emission re-radiated at infrared wavelengths by dust. Efficient reprocessing by dense gas and dust may explain the difference between theoretical predictions and observed luminosities of TDEs. The radio observations resolve an expanding and decelerating jet, probing the jet formation and evolution around a SMBH.

The tidal disruption of stars by supermassive black holes (SMBH) in the nuclei of galaxies was predicted theoretically thirty years ago (*1-2*). In a tidal disruption event (TDE), roughly half of the star's mass is ejected whereas the other half is accreted onto the SMBH, generating a bright flare that is normally detected at X-ray, ultraviolet (UV), and optical wavelengths *(3-5)*. TDEs are also expected to produce radio transients, lasting from months to years and including the formation of a relativistic jet, if a fraction of the accretion power is chanelled into a relativistic outflow *(6)*. TDEs provide a means of probing central black holes in quiescent galaxies and testing scenarios of accretion onto SMBHs and jet formation *(3,6)*.

On 2005 January 30, we discovered a bright transient in the near-infrared (IR) *(7)* coincident with the western nucleus B1 (Fig. 1) of the nearby [44.8 Mpc (*7*)] luminous infrared galaxy (LIRG) Arp 299. In galaxy mergers like Arp 299, large amounts of gas fall into the central regions, triggering a starburst. The long-term radio variability (*8*) and the IR spectral energy distribution (SED) (*9*) indicate a very high core-collapse supernova (SN) rate of ~0.3 yr^{-1} within the B1 nucleus. The B1 region also harbors a Compton-thick active galactic nucleus (AGN) that has been seen directly only in hard X-rays (*10*). This is consistent with an extremely high extinction A_V of ~ 460 magnitudes through an almost edge-on AGN torus (*11*). Galaxy mergers like Arp 299 are expected to have TDE rates several orders of magnitude higher than in field galaxies, albeit for relatively short periods of time [$\sim 3\times10^5$ yr (*12*)].

The transient source (henceforth Arp 299-B AT1) was discovered as part of a near-IR (2.2 μm) survey for highly obscured SNe in starburst galaxies (*13*). Over the following years it became luminous at IR and radio wavelengths, but was much fainter in the optical (*7*), implying substantial extinction by interstellar dust in Arp 299. Our follow-up observations show that the nuclear outburst had a peak brightness comparable to the entire galaxy nucleus at both near-IR and radio wavelengths (Fig. 4; *8*). Based on the energetics and multi-wavelength behavior of Arp 299-B AT1 over a decade of observations (Figs. 1-3), two broad scenarios to explain its origin are plausible: (i) an event unrelated to the SMBH, such as an extremely energetic SN, or a gamma-ray burst; or (ii) accretion-induced SMBH variability, such as an AGN flare, or a TDE.

High angular resolution [100 milliarcseconds (mas)], adaptive optics assisted, near-IR imaging observations from the Gemini-North telescope (*7*) show that Arp 299-B AT1 remained stationary and coincident (within 37 mas, corresponding to ~8 pc projected distance) with the near-IR *K*-band nucleus, as seen in pre-outburst imaging from the *Hubble* Space Telescope (*HST*) (Fig. 1). Radio observations obtained with very long baseline interferometry (VLBI) constrain its position with milliarcsecond angular precision (*7*). Pre-discovery Very Long Baseline Array (VLBA) observations showed several compact sources at 2.3 GHz within the central few parsecs of the B1 nucleus, but no counterparts at higher frequencies *(14)*. A new compact radio source was detected on 2005 July 17 at 8.4 GHz with the VLBA *(7, 14)*. The coincidence of the near-IR and VLBI positions, together with the appearance of the VLBI source soon after the near-IR detection and their subsequent evolution (see below; *7*), point to a common origin for both.

High angular resolution radio observations of Arp 299-B AT1 with VLBI show that the initially unresolved radio source developed a prominent extended, jet-like structure, which became evident in images taken from 2011 onwards (Fig. 1; *7*). The measured average apparent expansion speed of the forward shock of the jet is $(0.25\pm0.03)c$ between 2005 and 2015 *(7)*, where c is the speed of light. The radio morphology, evolution and expansion velocity of Arp 299-B AT1 rule out a SN origin. Similarly, a gamma-ray burst is inconsistent with both the observed peak flux density and time to reach that peak in the radio (*15*).

Therefore, the most likely explanation is that Arp 299-B AT1 is linked to an accretion event onto the SMBH. The persistent 2.3 GHz radio emission most likely corresponds to the quiescent AGN core (*7*).

The multi frequency radio light curves of Arp 299-B AT1 (Fig. 2) are well reproduced by a model (*16*) of a jet powered by accretion of part of a tidally disrupted star onto a SMBH (*7*). The jet initially moves at relativistic speeds ~0.995 *c*, but after a distance of less than $\sim 10^{17}$ cm (corresponding to ~760 days after the burst) it has already decelerated significantly to ~0.22 *c*, in agreement with expectations for TDE-driven jets *(6)*. The apparent speed of the jet indicated by the VLBI observations, together with the non-detection of the counterjet, constrains the jet viewing angle, θ_{obs}, to be within a narrow range: 25°-35° (*7*). If the jet had been launched by a pre-existing AGN, its viewing angle with respect to our line-of-sight should have been close to 90°, as the AGN torus is seen almost edge-on *(11),* and a counterjet should have also been detected *(7)*. However, a radio jet associated with a TDE does not necessarily have to be perpendicular to the pre-existing AGN accretion disc *(17)*. We therefore identify the observed radio jet as being launched by a TDE. While such jets have been predicted (*6*), no direct imaging has previously shown an expanding jet in a TDE, and its likely presence has been inferred based on radio observations only in the cases of ASASSN-14li (*18-19*), IGR J12580+0134 *(20),* and Swift J164449.3+573451 (hereafter Sw J1644+57; *21*). Our VLBI observations show a resolved, expanding radio jet in a TDE, in accordance with theoretical expectations *(6)*.

The intrinsic (i.e. beaming-corrected) kinetic energy of the jet required to reproduce the radio light curves (Fig. 2) is $(1.8 \pm 0.9) \times 10^{51}$ erg *(7)*, similar to the case of the relativistic TDE Sw J1644+57 (*16*). The rise of the radio emission at high frequencies in less than about 200 days and the significant delay of the lower-frequency radio emission (7) implies the existence of substantial external absorption, consistent with the jet being embedded in the very dense nuclear medium of the AGN, which has a constant number density $\sim 4 \times 10^4$ cm^{-3} up to a distance 6.3×10^{17} cm from the central engine (*7*).

Observations from the ground and the *Spitzer* Space Telescope show that the IR SED of Arp 299-B AT1 and its evolution from 2005 until 2016 can be explained by a single blackbody component (Fig. 3). The blackbody radius expands from 0.04 pc to 0.13 pc between May 2005 and Jan. 2012 while its temperature cools from ~1050 K to ~750 K. The size, temperature and peak luminosity (6×10^{43} erg s^{-1}) of the IR emitting region agrees well with both theoretical predictions and observations of thermal emission from warm dust surrounding TDEs *(22-23)*. Therefore, the IR SED and its evolution are consistent with absorption and re-radiation of the UV and optical light from Arp 299-B AT1 by local dust.

We modeled the IR SED of the pre- and post-outburst (734 days after the first IR detection) components of Arp 299-B1 using radiative transfer models for the emission from a starburst within the galaxy and a dusty torus predicted by the standard unified model for AGN, including also the effect of dust in the polar regions of the torus (Fig. 4, *24*). The model luminosities of the starburst and AGN dusty torus components remain constant within the uncertainties, whereas the luminosity of the polar dust component is found to increase by a factor of ~15 after the outburst, and the corresponding polar dust temperature increases from 500 to 900 K. Therefore, the observed IR SED of Arp 299-B AT1 can be most plausibly explained by re-radiation by optically thick dust clouds in the polar regions of the torus, which suffer from a relatively low foreground extinction within Arp 299-B1 (*7*).

Integrating the luminosity of Arp 299-B AT1 over the period 2005-2016 (Fig. 3) yields a total radiated energy of about 1.5×10^{52} erg. However, a significant fraction of the total energy emitted by the transient can be expected to be scattered, absorbed, and re-

radiated at substantially longer IR wavelengths by the dusty torus. We estimate that the fraction of energy that heated the polar dust was in the range 23%-78% (*7*). Thus the total radiated energy of Arp 299-B AT1 was $(1.9\text{-}6.5)\times10^{52}$ erg, which requires a disruption of a star with a mass of about 1.9-6.5 solar masses ($M_\odot$), assuming a standard accreted fraction and radiative efficiency (*7*). Stars in this mass range can be disrupted by the $\sim2\times10^7$ $M_\odot$ SMBH in Arp 299-B1 (*10, 25*). The kinetic energy of the jet is expected to be about 1% of the total energy *(6)*, which agrees well with our estimated kinetic energy for the radio jet of Arp 299-B AT1 *(7)*.

In addition to Arp 299-B AT1, the only other TDE candidates (with debated nature) to have an observed radiated energy on the order of 10^{52} erg are ASASSN-15lh (*26-27*) and possibly transients similar to PS1-10adi (*28*). While the high energy of ASASSN-15lh was proposed to be the result of a high mass (7.6×10^8 $M_\odot$), rapidly rotating black hole (27), in the case of PS1-10adi the large radiated energy was proposed to arise from the interaction of the expanding TDE material with the dense nuclear medium (*28*). Arp 299-B AT1 was most plausibly the result of the disruption of a star more massive than about 2 $M_\odot$ in a very dense medium. The soft X-ray photons produced by the event were efficiently reprocessed into ultraviolet and optical photons by the dense gas, and further to IR wavelengths by dust in the nuclear environment. Efficient reprocessing of the energy might thus resolve the outstanding problem of observed luminosities of optically detected TDEs being generally lower than predicted *(29)*.

The case of Arp 299-B AT1 suggests that recently formed massive stars are being accreted onto the SMBH in such environments, resulting in TDEs injecting large amounts of energy into their surroundings. However, events similar to Arp 299-B AT1 may remain hidden within dusty and dense environments, and would not be detectable by optical, UV or soft X-ray observations. The recent discovery of another TDE candidate in the nucleus of the luminous infrared galaxy IRAS F01004-2237 *(30)* yields further support for an enhanced rate of TDEs in such galaxies, which could be missed due to dust extinction. Such TDEs from relatively massive, newly formed stars might provide a large radiative feedback, especially at higher redshifts where galaxy mergers and LIRGs are more common (*31*).

References and Notes:

1. J. G. Hills, Possible power source of Seyfert galaxies and QSOs. *Nature* **254**, 295-298 (1975).
2. M. J. Rees. Tidal disruption of stars by black holes of 10^6-10^8 solar masses in nearby galaxies. *Nature* **333**, 523-528 (1988).
3. S. van Velzen et al. A radio jet from the optical and X-ray bright stellar tidal disruption flare ASASSN-14li. *Science*, **351**, 62-65 (2016).
4. B. A. Zauderer et al., Birth of a relativistic outflow in the unusual γ-ray transient Swift J164449.3+573451. *Nature*, **476**, 425-428 (2011).
5. S. Komossa. Tidal disruption of stars by supermassive black holes: Status of observations. *Journal of High Energy Astrophysics*, 7, 1**48-157** (2015).
6. D. Giannios and B. D. Metzger, Radio transients from stellar tidal disruption by massive black holes. *Mon. Not. R. Astron. Soc.* **416**, 2102-2107 (2011).
7. Materials and methods are available as supplementary materials on *Science* Online.
8. C. Romero-Cañizales et al. The core-collapse supernova rate in Arp 299 revisited. *Mon. Not. R. Astron. Soc.* **415**, 2688-2698 (2011).

9. S. Mattila et al. Core- collapse Supernovae Missed by Optical Surveys. *Astrophys. J.* **756**, 111 (2012).
10. A. Ptak et al. A Focused, Hard X-Ray Look at Arp 299 with NuSTAR. *Astrophys. J.* **800**, 104 (2015).
11. A. Alonso-Herrero et al. Uncovering the Deeply Embedded Active Galactic Nucleus Activity in the Nuclear Regions of the Interacting Galaxy Arp 299. *Astroph. J.,* **779L**, 14 (2013).
12. X. Chen, A. Sesana, P. Madau, F. K. Liu. Tidal Stellar Disruptions by Massive Black Hole Pairs. II. Decaying Binaries. *Astroph. J.,* **729**, 13 (2011).
13. S. Mattila et al. Arp 299. *IAU Circ.* **8477**, 2 (2005).
14. J.S. Ulvestad. Radio Emission from Young Supernovae and Supernova Remnants in Arp 299. *Astron. J.* **138**, 1529-1538 (2009).
15. P. Chandra, D. A. Frail. A Radio-selected Sample of Gamma-Ray Burst Afterglows. *Astrophys. J.* **746**, 156 (2012).
16. P. Mimica, D. Giannios, B. D. Metzger, M. A. Aloy. The radio afterglow of Swift J1644+57 reveals a powerful jet with fast core and slow sheath. *Mon. Not. R. Astron. Soc.* **450**, 2824 (2015).
17. S. Rosswog, E. Ramirez-Ruiz, W. R. Hix. Tidal Disruption and Ignition of White Dwarfs by Moderately Massive Black Holes. *Astrophys. J.* **695**, 404 (2009).
18. C. Romero-Cañizales et al. The TDE ASASSN-14li and Its Host Resolved at Parsec Scales with the EVN. *Astrophys. J.* **832L**, 10 (2016).
19. K. D. Alexander, E. Berger, J. Guillochon, B. A. Zauderer, P. K. G. Williams. Discovery of an Outflow from Radio Observations of the Tidal Disruption Event ASASSN-14li. *Astroph. J.* **819**, L25 (2016).
20. E. S. Perlman et al. Compact Resolved Ejecta in the Nearest Tidal Disruption Event. *Astrophys. J.* **842**, 126 (2017).
21. J. Yang et al. No apparent superluminal motion in the first-known jetted tidal disruption event Swift J1644+5734. *Mon. Not. R. Astron. Soc.* **462**, 66L (2016).
22. S. van Velzen, A.J. Mendez, J.H. Krolik, V. Gorjian. Emission from Dust Heated by Stellar Tidal Disruption Flares. *Astrophys. J.* **829**, 19 (2016).
23. L. Dou et al. Discovery of a Mid-infrared Echo from the TDE Candidate in the Nucleus of ULIRG F01004-2237. *Astrophys. J.* **841L**, 8 (2017).
24. A. Efstathiou. A model for the infrared emission of FSC 10214+4724. *Mon. Not. R. Astron. Soc.* **371**, L70 (2006).
25. J. Law-Smith et al. Low-mass White Dwarfs with Hydrogen Envelopes as a Missing Link in the Tidal Disruption Menu. *Astrophys. J.* **841**, 132L (2017).
26. S. Dong et al. ASASSN-15lh: A highly super-luminous supernova. *Science* **351**, 257-260 (2016).
27. G. Leloudas et al. The Superluminous Transient ASASSN-15lh as a Tidal Disruption Event from a Kerr Black Hole. *Nature Astron.*,**1**, 0002 (2016).
28. E. Kankare et al. A population of highly energetic transient events in the centres of active galaxies. *Nature Astron.*,**1**, 0865 (2017).
29. T. Piran, G. Svirski, J. Krolik, R. M. Cheng, H. Shiokawa. Disk Formation Versus Disk Accretion—What Powers Tidal Disruption Events? *Astrophys. J.*, **806**, 164 (2015).
30. C. Tadhunter, R. Spence, M. Rose, J. Mullaney, P. Crowther. A tidal disruption event in the nearby ultra-luminous infrared galaxy F01004-2237. *Nature Astron.*, 1, 61 (2017).

31. B. Magnelli et al. The deepest Herschel-PACS far-infrared survey: number counts and infrared luminosity functions from combined PEP/GOODS-H observations. *Astron. & Astrophys. Suppl.* **553**, 132 (2013).
32. R. Ma, F.-G. Xie, S. Hou. Relationship between the Kinetic Power and Bolometric Luminosity of Jets: Limitation from Black Hole X-Ray Binaries, Active Galactic Nuclei, and Gamma-Ray Bursts. *Astrophys. J.*, **780L**, 14 (2017).
33. Z.Y. Huo, X.Y. Xia, S.J. Xue, S. Mao, & Z.G. Deng. Chandra Observations of Ultraluminous Infrared Galaxies: Extended Hot Gaseous Halos in Merging Galaxies *Astrophys. J.* **611**, 208 (2004).
34. D.B. Sanders, J.M. Mazzarella, D.C Kim, J.A. Surace, B.T. Soifer. The IRAS Revised Bright Galaxy Sample. *Astron. J.* **126**, 1607 (2003).
35. J. E. Hibbard, M. S. Yun. A 180 Kiloparsec Tidal Tail in the Luminous Infrared Merger ARP 299. *Astron. J.* **118**, 162-185 (1999).
36. R. Della Ceca et al. An Enshrouded Active Galactic Nucleus in the Merging Starburst System Arp 299 Revealed by BeppoSAX. *Astrophys. J.* **581L**, 9 (2002).
37. S. Mattila, W. P. S Meikle. Supernovae in the nuclear regions of starburst galaxies. *Mon. Not. R. Astron. Soc.* **324**, 325-342 (2001).
38. S. Mattila, W. P. S. Meikle, R. Greimel. Highly extinguished supernovae in the nuclear regions of starburst galaxies. *New Astron. Rev.* **48**, 595 (2004).
39. C. Packham et al. INGRID: A near-infrared camera for the William Herschel Telescope. *Mon. Not. R. Astron. Soc.* **345**, 395 (2003).
40. A. Manchado et al. LIRIS: a long-slit intermediate-resolution infrared spectrograph for the WHT. Proc. SPIE, ed. A.M. Fowler, **3354**, 448 (1998).
41. D. Tody. The *IRAF* Data Reduction and Analysis System. Proc. SPIE, ed. D.L. Crawford, **627**, 733 (1986).
42. C. Alard, R.H. Lupton. A method for Optical Image Subtraction. *Astrophys. J.*, **503**, 325 (1998).
43. C. Alard et al. Image subtraction using a space-varying kernel. *Astron. & Astrophys. Suppl.* **144**, 363 (2000).
44. S. Mattila et al. Supernovae 2005Q, 2005R, 2005S, 2005T, 2005U. *IAU Circ.* **8473**, 1 (2005).
45. J.B. Oke, J.E. Gunn. Secondary standard stars for absolute spectrophotometry. *Astrophys. J.*, **266**, 713 (1983).
46. B. Abolfathi et al. The Fourteenth Data Release of the Sloan Digital Sky Survey: First Spectroscopic Data from the extended Baryon Oscillation Spectroscopic Survey and from the second phase of the Apache Point Observatory Galactic Evolution Experiment. *arXiv:* 1707.09322 (2017).
47. J.A. Holtzman et al. The Photometric Performance and Calibration of WFPC2. Publ. of the Astron. Soc. of the Pac. **107**, 1065 (1995).
48. M. Sirianni et al. The Photometric Performance and Calibration of the Hubble Space Telescope Advanced Camera for Surveys. Publ. of the Astron. Soc. of the Pac. **117**, 1049 (2005).
49. R.A. Kimble et al. Wide Field Camera 3: a powerful new imager for the Hubble Space Telescope. Proc. SPIE. Vol. **7010**, 12 (2008).
50. A. Becker. HOTPANTS: High Order Transform of PSF ANd Template Subtraction. *Astrophysics Source Code Library*, ascl:1505.004 (2015).
51. S. Gonzaga, et al. ACS Data Handbook v. 7.2, Baltimore, STScI (2014).
52. A. Rajan et al. WFC3 Data Handbook v. 2.1, Baltimore: STScI (2011).

53. P.F. Roche et al. UFTI: the 0.8 - 2.5 μm fast track imager for the UK infrared telescope. Proc. SPIE, Vol. **4841**, 901-912 (2003).
54. T.M Abbott, C. Aspin, A.N. Sorensen et al. SWIR at the Nordic Optical Telescope: NOTCam. Proc. SPIE, Vol. **4008**, 14-719 (2000).
55. E. Kankare et al. The nature of supernovae 2010O and 2010P in Arp 299 - I. Near-infrared and optical evolution. *Mon. Not. R. Astron. Soc.* **415**, 2688-2698 (2014).
56. M.A. Shure, D.W. Toomey, J.T. Rayner, P.M. Onaka & A.J. Denault. NSFCAM: a new infrared array camera for the NASA Infrared Telescope Facility. Proc. SPIE, Vol. **2198**, 614-622 (1994).
57. W. Wu, G.C. Clayton, K.D. Gordon et al. A New Database of Observed Spectral Energy Distributions of Nearby Starburst Galaxies from the Ultraviolet to the Far-Infrared. *Astroph. J. Suppl,* **134**, 377 (2002).
58. M. F. Skrutskie et al. The Two Micron All Sky Survey (2MASS). *Astron. J.,* **131**, 1163 (2006).
59. P. W. Draper, N. Gray, D. Berry and M. Taylor. Starlink User Note 214.44. Starlink project (2014). http://star-www.rl.ac.uk/docs/sun214.htx/sun214.html
60. R. Thompson. NICMOS - Near-Infrared Camera and Multi-Object Spectrometer. Space Science Rev. (ISSN 0038-6308), vol. **61**, 1-2, 69-93 (1992).
61. A. Alonso-Herrero, G. H. Rieke, M. J. Rieke, N. Z. Scoville. Extreme Star Formation in the Interacting Galaxy Arp 299 (IC 694+NGC 3690). *Astrophys. J.*, **532**, 845 (2000).
62. G.G. Fazio, J.L. Hora, L.E. Allen et al. The Infrared Array Camera (IRAC) for the Spitzer Space Telescope. *Astroph. J. Suppl,* **154**, 10 (2004).
63. S. Laine (Ed). IRAC Instrument Handbook v. 2.1.2 (2015).
64. M. A. Pérez-Torres, C. Romero-Cañizales, A. Alberdi, A., An extremely prolific supernova factory in the buried nucleus of the starburst galaxy IC 694. *Astron. Astrophys.* **507**, L17 (2009).
65. M. Bondi, M. A. Pérez-Torres, R. Herrero-Illana, A. Alberdi, A., The nuclear starburst in Arp 299-A: from the 5.0 GHz VLBI radio light-curves to its core-collapse supernova rate. *Astron. Astrophys.* **539**, A134 (2012).
66. E. Greisen. AIPS, the VLA, and the VLBA. in *Information Handling in Astronomy - Historical Vistas*, André Heck, Ed. (Kluwer Academic Publishers, 2003) *Astroph. and Space Science Library,* vol. **285**, p. 109.
67. M. Kettenis, H.-J. van Langevelde, C. Reynolds, and B. Cotton, in *Astronomical Data Analysis Software and Systems XV*, Carlos Gabriel et al., Ed. (Astronomical Society of the Pacific, San Francisco, 2006), vol. **351**, p. 497 (2006).
68. D. S. Briggs. High-fidelity deconvolution of moderately resolved sources. Ph.D. Thesis, New Mexico Institute of Mining and Technology, Socorro, New Mexico (1995).
69. A. Fruscione, J.C. McDowell, G.E. Allen et al. CIAO: Chandra's data analysis system. Proc. SPIE, Vol. **6270**, 62701V (2006).
70. https://heasarc.gsfc.nasa.gov/docs/heasarc/caldb/docs/memos/cal_gen_94_002/cal_gen_94_002.html
71. K.A. Arnaud. XSPEC: The First Ten Years. Astronomical Data Analysis Software and Systems. Vol, **101**, 17 (1996).
72. K. Anastasopoulou, A. Zezas, L. Ballo, R. Della Ceca. A deep Chandra observation of the interacting star-forming galaxy Arp 299. *Mon. Not. R. Astron. Soc.* **460**, 3570 (2016).
73. T. Krühler et al. GRB hosts through cosmic time. VLT/X-Shooter emission-line

spectroscopy of 96 γ-ray-burst-selected galaxies at $0.1 < z < 3.6$. *Astron. & Astrophys.* **581**, 125 (2015).
74. J. P. Anderson, S. M. Habergham, P. A. James. On the multiple supernova population of Arp 299: constraints on progenitor properties and host galaxy star formation characteristics. *Mon. Not. R. Astron. Soc.* **416**, 567 (2011).
75. J. M. Marcaide, I. I. Shapiro. VLBI study of 1038 + 528 A and B - Discovery of wavelength dependence of peak brightness location. *Astroph. J.,* **276**, 56 (1984).
76. A. B. Pushkarev et al. MOJAVE: Monitoring of Jets in Active galactic nuclei with VLBA Experiments. IX. Nuclear opacity. *Astron. & Astrophys.* **545**, A113 (2012).
77. P. Mimica et al. Spectral Evolution of Superluminal Components in Parsec-Scale Jets. *Astroph. J.,* **696**, 1142 (2009).
78. P. Mimica, M.A. Aloy, D. Giannios, B.D. Metzger. Numerical simulations of the jetted tidal disruption event Swift J1644+57. Journal of Physics Conference Series, **719**, 012008 (2016).
79. M. A. Aloy, J. M. Ibanez, J. M. Marti, E. Muller. GENESIS: A High-Resolution Code for Three-dimensional Relativistic Hydrodynamics. *Astroph. J. S. S.* **152**, 151 (1999).
80. P. Mimica, D. Giannios, M. A. Aloy. Deceleration of arbitrarily magnetized GRB ejecta: the complete evolution. *Astron. Astroph.,* **494**, 879 (2009).
81. C. M. Urry, P. Padovani. Unified Schemes for Radio-Loud Active Galactic Nuclei. *Publications of the Astronomical Society of the Pacific.* **107**, 803 (1995).
82. D. Foreman-Mackey, D. W. Hogg, D. Lang, J. Goodman. emcee: The MCMC Hammer. *Publications of the Astronomical Society of the Pacific.* **125**, 306 (2013).
83. S. Kozlowski et al. SDWFS-MIT-1: A self-obscured luminous supernova at $z \sim= 0.2$. *Astroph. J.,* **722**, 1624 (2010).
84. M. Xue et al. A Precise Determination of the Mid-infrared Interstellar Extinction Law Based on the APOGEE Spectroscopic Survey. *Astroph. J. Suppl,* **224**, 23 (2016).
85. J. A. Cardelli, G. C. Clayton, J. S. Mathis. The relationship between infrared, optical, and ultraviolet extinction. *Astroph. J.,* **345**, 245 (1989).
86. V. P. Utrobin. An optimal hydrodynamic model for the normal type IIP supernova 1999em. *Astron. & Astrophys.* **461**, 233 (2007).
87. R. R. J. Antonucci, J.S. Miller. Spectropolarimetry and the nature of NGC 1068. *Astroph. J.,* **297**, 621 (1985).
88. S. F. Hönig et al. Dust in the Polar Region as a Major Contributor to the Infrared Emission of Active Galactic Nuclei. *Astroph. J.,* **771**, 87 (2013).
89. M. García-Marín, L. Colina, S. Arribas, A. Alonso-Herrero, E. Mediavilla. Integral Field Spectroscopy of the Luminous Infrared Galaxy Arp 299 (IC 694 + NGC 3690). *Astroph. J.,* **650**, 850 (2006).
90. http://ahpc.euc.ac.cy/index.php/resources/cygnus
91. A. Efstathiou & R. Siebenmorgen. Starburst and cirrus models for submillimeter galaxies. *Astron. & Astrophys.* **502**, 541 (2009).
92. A. Efstathiou, M. Rowan-Robinson, R. Siebenmorgen. Massive star formation in galaxies: radiative transfer models of the UV to millimetre emission of starburst galaxies. *Mon. Not. R. Astron. Soc.* **313**, 734 (2000).
93. G. Bruzual, S. Charlot. Stellar population synthesis at the resolution of 2003. *Mon. Not. R. Astron. Soc.* **344**, 1000 (2003).
94. A. Efstathiou, M. Rowan-Robinson. Dusty discs in active galactic nuclei. *Mon. Not. R. Astron. Soc.* 273, **649** (1995).
95. A. Efstathiou, J. H. Hough, S. Young. A model for the infrared continuum spectrum of

NGC 1068. *Mon. Not. R. Astron. Soc.* **277**, 1134 (1995).
96. S. P. Johnson, G. W. Wilson, Y. Tang, K. S. Scott. SATMC: Spectral energy distribution analysis through Markov Chains. *Mon. Not. R. Astron. Soc.* **436**, 2354 (2013).
97. K. Hryniewicz, R. Walter. Unbeamed tidal disruption events at hard X-rays. *Astron. & Astrophys.* **586**, 9 (2016).
98. F. Vagnetti, S. Turriziani, D. Trevese. Ensemble X-ray variability of active galactic nuclei from serendipitous source catalogues. *Astron. & Astrophys.* **536**, 84 (2011).
99. B. D. Metzger & N. C. Stone. A bright year for tidal disruptions. *Mon. Not. R. Astron. Soc.* 461, 948 (2016).

Acknowledgements

Acknowledgements:
We thank Andrew Fabian, Talvikki Hovatta, Andrew Levan, Kari Nilsson and Claudio Ricci for useful discussions. We also thank the anonymous referees for many insightful comments which have improved the manuscript. Our findings are based mainly on observations obtained with the Spitzer Space Telescope, the European VLBI Network, the Very Long Baseline Array and Very Large Array, the Nordic Optical Telescope (NOT), and the Gemini Observatory. The Spitzer Space Telescope is operated by the Jet Propulsion Laboratory, California Institute of Technology under a contract with NASA. The European VLBI Network is a joint facility of independent European, African, Asian, and North American radio astronomy institutes. The National Radio Astronomy Observatory is a facility of the National Science Foundation operated under cooperative agreement by Associated Universities, Inc. The Nordic Optical Telescope is operated by the Nordic Optical Telescope Scientific Association at the Observatorio del Roque de los Muchachos, La Palma, Spain, of the Instituto de Astrofisica de Canarias. The Gemini Observatory is operated by the Association of Universities for Research in Astronomy, Inc., under a cooperative agreement with the NSF on behalf of the Gemini partnership: the National Science Foundation (United States), the National Research Council (Canada), CONICYT (Chile), Ministerio de Ciencia, Tecnología e Innovación Productiva (Argentina), and Ministério da Ciência, Tecnologia e Inovação (Brazil). Figure 1 image credit: NASA, ESA, the Hubble Heritage Team (STScI/AURA)-ESA/Hubble Collaboration and A. Evans (University of Virginia, Charlottesville/NRAO/Stony Brook University).

Funding:
SM acknowledges financial support from the Academy of Finland (project: 8120503). The research leading to these results has received funding from the European Commission Seventh Framework Programme (FP/2007-2013) under grant agreement numbers 227290, 283393 (RadioNet3) and 60725 (HELP). AA, MAPT, NRO and RHI acknowledge support from the Spanish MINECO through grants AYA2012-38491-C02-02 and AYA2015-63939-C2-1-P. PGJ acknowledges support from European Research Council Consolidator Grant 647208. C.R.-C. acknowledges support by the Ministry of Economy, Development, and Tourism's Millennium Science Initiative through grant IC120009, awarded to The Millennium Institute of Astrophysics, MAS, Chile and from CONICYT through FONDECYT grant 3150238 and China-CONICYT fund CAS160313. PM and MAA

acknowledge the support from the ERC research grant CAMAP-250276, and the partial support from the Spanish MINECO grant AYA2015-66889-C2-1P and the local Valencia government grant PROMETEO-II-2014-069. MF acknowledges support from a Science Foundation Ireland - Royal Society University Research Fellowship. DC acknowledges the support from the grants ST/G001901/1, ST/J001368/1, ST/K001051/1, ST/N000838/1.

Author contributions:
SM and MPT co-led the writing of the manuscript, the data analysis and physical interpretation. AE modeled the IR SED and contributed to the physical interpretation and text. PM and MAA modeled the radio light curves and contributed to the physical interpretation and text. MF analysed the HST data and contributed to the physical interpretation and text. EK contributed to the observations and analysis of the near-IR data, the physical interpretation and text. AA, CRC, and IMV contributed to the analysis and interpretation of the radio data, and text. EV, MB, RHI, NRO, RB and KW contributed to the analysis and interpretation of the radio data. TH and ST analysed the X-ray data. PJ and SS contributed to the physical interpretation and text. PL and CF contributed to the physical interpretation. AAH, WM, RK and PV contributed to the analysis and physical interpretation of the infrared data. JH, TK and TR contributed to the observations and analysis of the near-IR data. DC, JK, KN, RG, SR, NW and GÖ contributed data. All co-authors contributed with comments to the text.

Competing interests:
We declare that none of the authors have any competing interest.

Data and materials availability:
The raw observations used in this publication are available from the Spitzer Heritage Archive at http://sha.ipac.caltech.edu/applications/Spitzer/SHA/ (Proposal IDs: 32, 108, 60142, 80105, 90031, 90157, 10086, 11076), from the EVN data archive at http://archive.jive.nl/scripts/listarch.php (proposal IDs EP063, EP068, EP075, EP087, GP053), the NRAO data archive at https://archive.nrao.edu/archive/advquery.jsp, from the NRAO data archive at https://archive.nrao.edu/archive/advquery.jsp (proposal IDs: BPU027, BP202, AC0749), the NOT data archive at http://www.not.iac.es/archive/, the Gemini Observatory Archive at https://archive.gemini.edu/searchform (programs: GN-2008B-Q-32, GN-2009A-Q-12, GN-2009B-Q-23, GN-2010A-Q-40, GN-2011A-Q-48 and GN-2011B-Q-73), the Hubble Legacy Archive at https://hla.stsci.edu/hlaview.html, the Chandra Data Archive at http://cxc.harvard.edu/cda/ (OBSIDs 1641, 6227, 15077 and 15619), the XMM-Newton Science Archive at http://nxsa.esac.esa.int/nxsa-web/ (ObsId 0679381101), the Isaac Newton Group Archive at http://casu.ast.cam.ac.uk/casuadc/ingarch/query, the United Kingdom Infrared Telescope Archive at http://casu.ast.cam.ac.uk/casuclient/ukirt_arch/, The radiative transfer models used in this paper are part of the CYGNUS project with the model grids available at http://ahpc.euc.ac.cy/index.php/resources/cygnus. The results of the hydrodynamic and radiative simulations used for modeling the radio light curves are available at https://www.uv.es/mimica/doc, as well as the data and Python code used to produce Fig. 2A and Fig. S6. The Python code used for determining the allowed values for the viewing angle of the radio jet and producing Fig. S7 is available at https://github.com/mapereztorres/rad-trans-theta. Full details of all data and software used in this paper are given in the supplementary material.

Supplementary Materials
www.sciencemag.org
Materials and Methods
Figs. S1 to S7
Tables S1 to S7
References (33-99) [Note: The numbers refer to any additional references cited only within the Supplementary Materials]

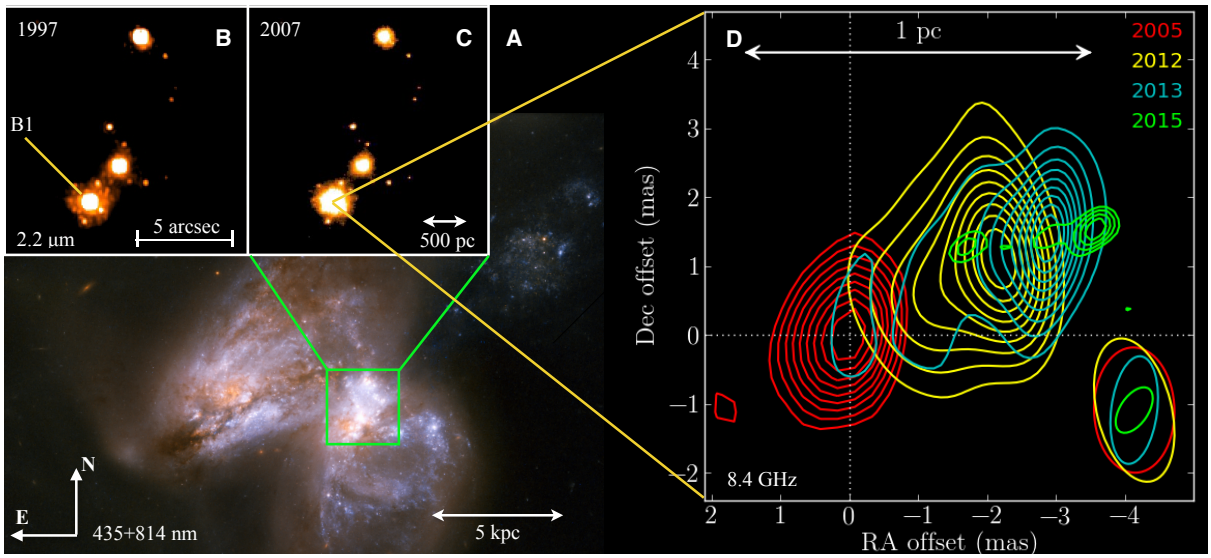

Figure 1. The transient Arp 299-B AT1 and its host galaxy Arp 299. (**A**) A color-composite optical image from the Hubble Space Telescope (*HST*), with high resolution, 12.5×13 arcsecond sized near-infrared 2.2 μm images (insets **B** and **C**) showing the brightening of the B1 nucleus (*7*). (**D**) The evolution of the radio morphology as imaged with Very Long Baseline Interferometry (VLBI) at 8.4 GHz (7×7 milliarcsecond region centered at the 8.4 GHz peak position in 2005, RA = 11h28m30.9875529s, Dec = 58°33′40″.783601 (J2000.0), indicated by the dotted lines). The VLBI images are aligned with an astrometric precision better than 50 μas. The initially unresolved radio source develops into a resolved jet structure a few years after the explosion, with the center of the radio emission moving westward with time (*7*). The radio beam size for each epoch is indicated in the lower-right corner.

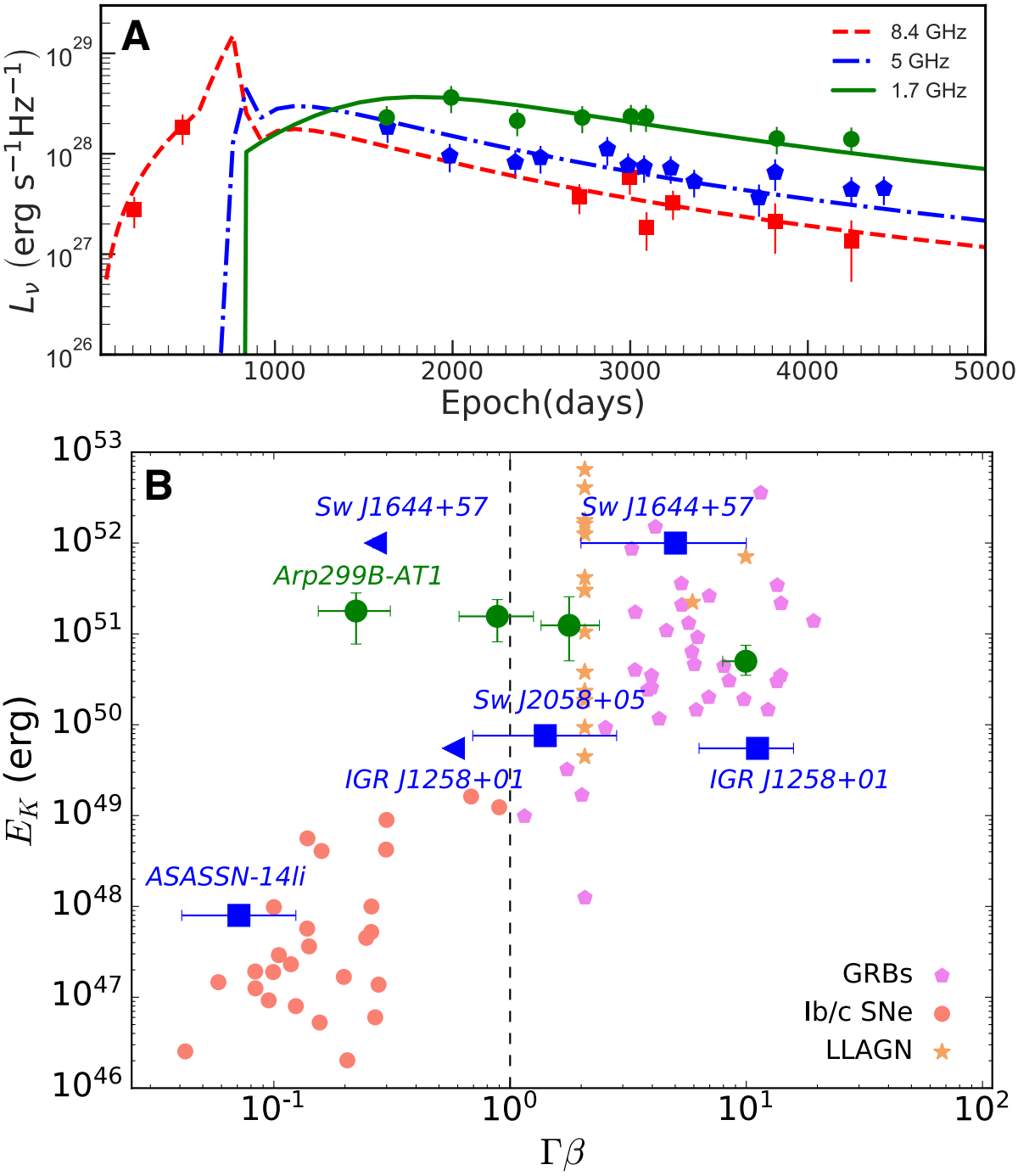

Figure 2. Radio properties of Arp 299-B AT1. (A) Radio luminosity, L_ν, evolution of Arp 299-B AT1 at 1.7 (circles), 5.0 (pentagons) and 8.4 GHz (squares) spanning more than 12.1 years of observations, along with modeled radio light curves, using hydrodynamic and radiative simulations for a tidal disruption event (TDE) launched jet *(16)*. The day zero corresponds to 2004 Dec. 21.6. **(B)** Intrinsic (beaming-corrected) jet kinetic energy, E_K, versus outflow speed ($\Gamma\beta$, where $\Gamma = (1-\beta^2)^{-1/2}$ is the bulk Lorentz factor of the outflow and $\beta = v/c$), from radio observations of gamma-ray bursts (GRB), supernovae (SNe), low-luminosity active galactic nuclei (LLAGN), and TDEs *(4, 16, 19-21, 32)*. The large circles show the inferred loci for Arp 299-B AT1 at four epoch from right to left: just after the jet is launched by the TDE, ~1, ~12, and ~760 days thereafter (in the observer frame). For the LLAGN sample, we have assumed a constant jet kinetic power over 10 yr. The triangles indicate upper limits for the expansion speed of IGR J1258+01 *(20)* and Sw J1644+57 *(21)*.

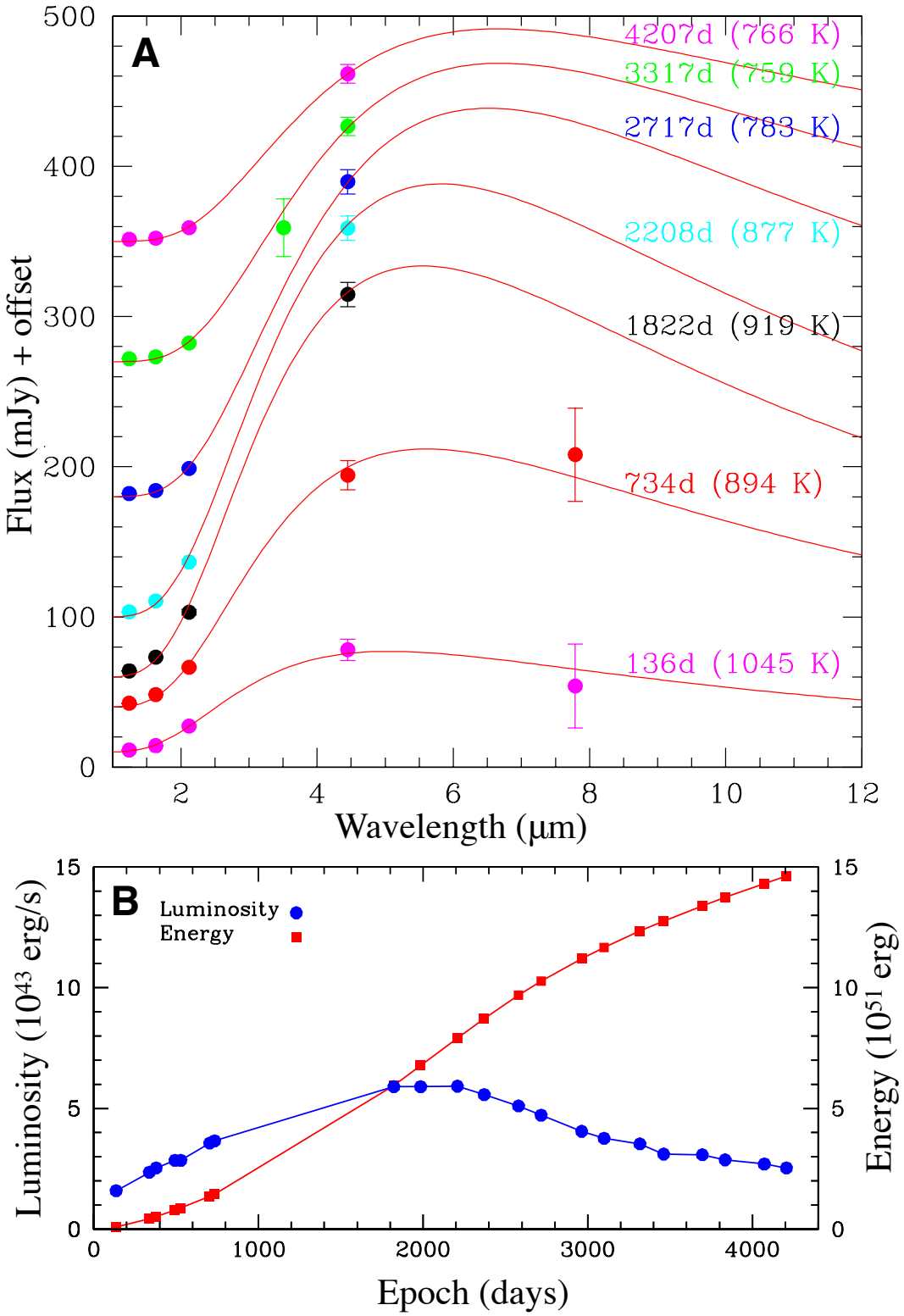

Figure 3. Infrared properties of Arp 299-B AT1. (A) The evolution of the observed infrared spectral energy distribution (points) shown together with blackbody fits between 136 and 4207 days after the first infrared detection on 2004 Dec. 21.6 (*7*). Over this period the blackbody temperature decreased from about 1050 to 750 K while the blackbody radius increased from 0.04 to 0.13 pc. **(B)** The evolution of the integrated blackbody luminosity (blue circles) and cumulative radiated energy (red squares). The observed radiated energy by day 4207 was about 1.5×10^{52} erg.

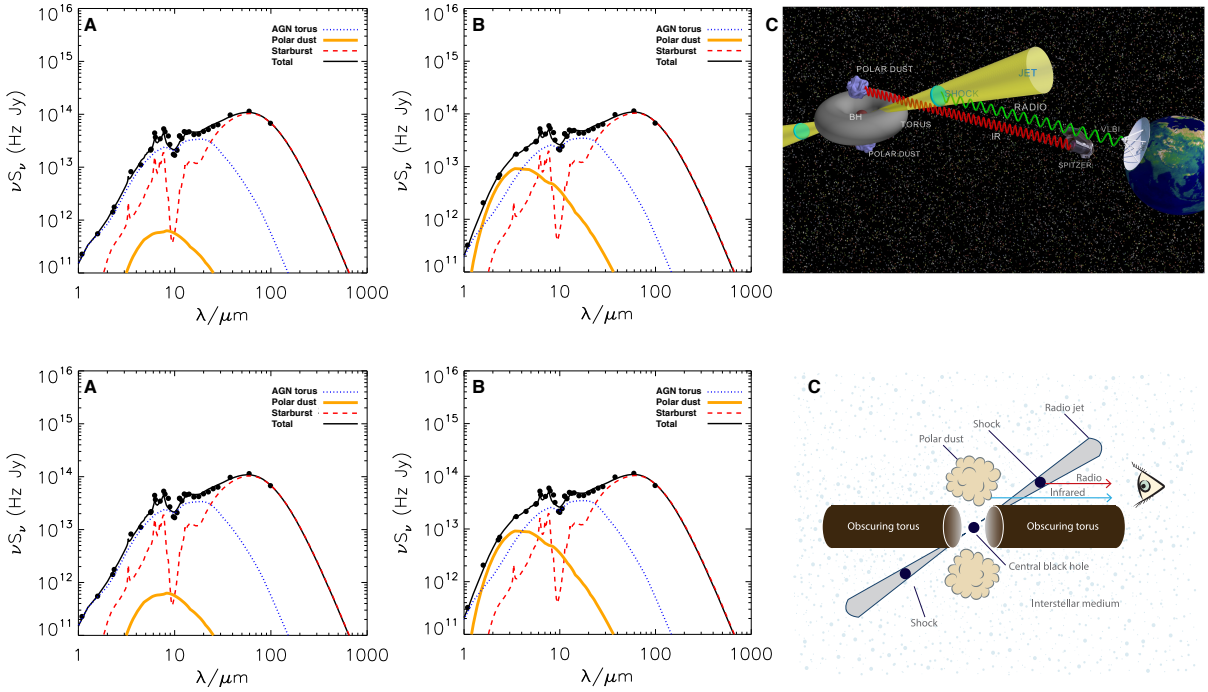

TWO ALTERNATIVE FIGURES ARE SHOWN

Figure 4. Model for the observed properties of Arp 299-B AT1. Shown are the best fitting models for the pre-outburst **(A)** and the post-outburst (734 days after the first mid-infrared detection) spectral energy distribution of the Arp 299 nucleus B **(B)**, with a starburst component (dashed line), an active galactic nucleus (AGN) dusty torus (dotted line), and a polar dust component (thick solid line) (*7*). The sum of these components is shown as a thin solid line. In **(B)** most of the model parameters were fixed, whilst the temperature of the polar dust varied from 500 K in the pre-outburst case to 900 K in the post-outburst case. This yields a covering factor of the polar dust of 23%-78%, implying that the total radiated energy is ~(1.9-6.5) $\times 10^{52}$ erg. **(C)** Schematic diagram (not to scale) showing the geometry of the emitting and absorbing regions (*7*). The tidal disruption event generates prominent X-ray, ultraviolet and optical emission. However, the direct line-of-sight to the central black hole is obscured by the dusty torus, which is opaque from soft X-rays to infrared wavelengths. The polar dust re-radiates in the infrared a fraction of the total energy emitted by the event. The transient radio emission originates from a relativistic jet launched by the tidal disruption of a star.